

Synthesis and Characterization of Poly(vinylidene fluoride) with Grafted Acid/Base Polymer Side Chains

Guangqun Zhai, Lei Ying, E. T. Kang,* and K. G. Neoh

Department of Chemical and Environmental Engineering, National University of Singapore, Kent Ridge, Singapore 119260

Received June 6, 2002; Revised Manuscript Received October 7, 2002

ABSTRACT: Thermally-induced molecular graft copolymerization of 4-vinylpyridine (4VP) with the ozone-preactivated poly(vinylidene fluoride) (PVDF) was carried out in *N*-methyl-2-pyrrolidone (NMP) solution to produce the 4VP-*g*-PVDF copolymer. The resulting 4VP-*g*-PVDF copolymers with different graft concentrations of the base polymer side chains were cast into microfiltration (MF) membranes by phase inversion. When compared to the MF membranes prepared from PVDF with grafted acrylic acid (AAc) polymer side chains from the earlier work, the 4VP-*g*-PVDF MF membranes also exhibited pH-sensitive permeability to aqueous solutions, but in an opposite manner. The fabrication of membranes from functional graft copolymers represented a relatively simple and effective approach to the preparation of membranes with well-controlled pore size, uniform surface, and pore–surface composition, and pH-sensitive flux properties.

Introduction

Because of its chemical inertness and good processability, poly(vinylidene fluoride) (PVDF) has been extensively investigated for its application as a membrane material.^{1–3} For certain applications, such as biofiltration and controlled drug release and delivery, membranes are required to respond to the changes in chemical environment, such as changes in pH value.⁴ In the absence of environmental sensitivity, the applicability of PVDF membranes in these areas will be limited. It is well-known that pH sensitivity exists within those polymers that contain acidic or basic functional groups. Surface modification by graft copolymerization of monomers containing these functional groups on existing membranes has been shown to be a convenient method to incorporate pH sensitivity.^{5–7}

However, surface modification of existing membranes by grafting or graft copolymerization is likely to be accompanied by changes in the membrane pore dimension and pore size distribution, leading to reduced permeability.^{8,9} Moreover, the extents of grafting on the membrane surfaces and the surfaces of the pores may differ considerably. Thus, the approach of molecular or bulk graft copolymerization, followed by phase inversion, to membrane fabrication may prove to be particularly useful in certain cases. For example, uniform post-functionalization by graft copolymerization of the hollow fiber membranes and their pore surfaces is expected to be spatially difficult. Earlier studies have described the graft copolymerization of acrylic acid¹⁰ and vinylpyridine¹¹ with PVDF. Furthermore, a recent study has shown that preparation of microfiltration membranes from PVDF with grafted acrylic acid side chains (the AAc-*g*-PVDF copolymers) by the phase inversion technique can greatly facilitate the control of the pore size, the pore size distribution and the composition of the pore surfaces through the control of the copolymer structure and composition.¹² In this report, we extend the study to the synthesis and characterization of PVDF

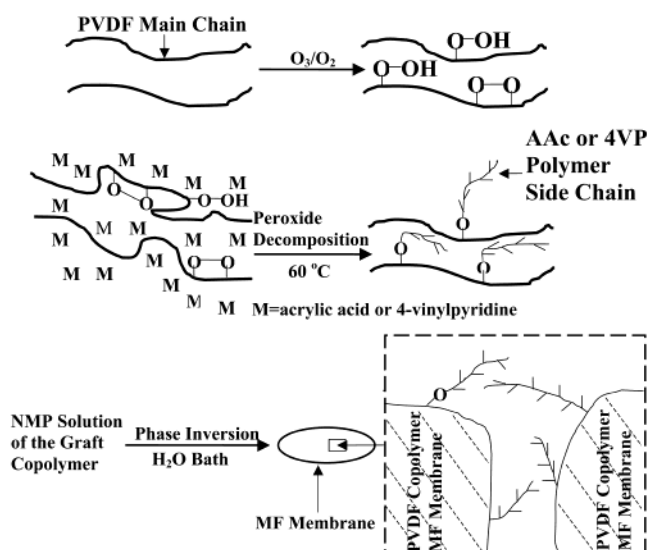


Figure 1. Schematic illustration of the processes of thermally induced graft copolymerization of AAc and 4VP on the ozone-preactivated PVDF backbones in solution and the preparation of the AAc-*g*-PVDF and 4VP-*g*-PVDF MF membranes by phase inversion.

with grafted base polymer side chains, viz., the 4-vinylpyridine (4VP) polymer side chains. The resulting 4VP-*g*-PVDF copolymers can be cast into microfiltration (MF) membranes by the phase inversion technique. The processes are shown schematically in Figure 1. The AAc-*g*-PVDF and 4VP-*g*-PVDF MF membranes exhibit pH-sensitive permeability to aqueous solutions, but in an opposite manner.

Experimental Section

The 4VP-*g*-PVDF copolymers were prepared by thermally induced molecular graft copolymerization of 4VP (Aldrich Chem. Co., Milwaukee, WI) with the ozone preactivated PVDF (Elf Atochem of North America Inc., Tacoma, WA) at $60^\circ C$ in *N*-methyl-2-pyrrolidone (NMP) solution under an argon atmosphere. The procedures were similar to those reported earlier for the preparation of the AAc-*g*-PVDF copolymers.¹²

* To whom all correspondence should be addressed. Fax: (65)-6779-1936. E-mail: cheket@nus.edu.sg.

Table 1. Bulk and Surface Graft Concentration and Mean Pore Size of the 4VP-*g*-PVDF and AAc-*g*-PVDF Copolymer Membranes as a Function of the Monomer Feed Ratio

$[4VP]/[-CH_2CF_2-]^a$ [AAc]/ $[-CH_2CF_2-]^b$ molar feed ratio	$([N]/[C])_{bulk}$ $([C]/[F])_{bulk}$	$([N]/[C])_{surface}$ $([C]/[F])_{surface}$	$([-4VP-]/[-CH_2CF_2-])_{bulk}$ $([-AAc-]/[-CH_2CF_2-])_{bulk}$	$([-4VP-]/[-CH_2CF_2-])_{surface}$ $([-AAc-]/[-CH_2CF_2-])_{surface}$	mean pore size ^c (μm)
0.61^a	0.02	0.05	0.04	0.13	0.95
<i>3.0^b</i>	<i>1.01</i>	<i>1.20</i>	<i>0.01</i>	<i>0.13</i>	<i>1.67</i>
1.22	0.02	0.08	0.04	0.32	1.03
<i>4.0</i>	<i>1.05</i>	<i>1.52</i>	<i>0.03</i>	<i>0.35</i>	<i>1.63</i>
3.05	0.03	0.09	0.07	0.55	1.31
<i>5.0</i>	<i>1.15</i>	<i>2.04</i>	<i>0.10</i>	<i>0.69</i>	<i>1.56</i>
3.66	0.04	0.10	0.08	0.68	1.38
<i>6.0</i>	<i>1.30</i>	<i>2.44</i>	<i>0.20</i>	<i>0.97</i>	<i>1.52</i>

^a The data in bold are for the 4VP-*g*-PVDF membranes. ^b The data in italic are for the AAc-*g*-PVDF membranes and were obtained from ref 12. ^c For microfiltration membranes cast from 12 wt % copolymer solutions by phase inversion. For commercial PVDF membranes with standard pore diameters of $d = 0.45$ and 0.65 μm, the mean pore size are 1.41 and 1.96 μm, respectively.

The bulk composition of the graft copolymers was characterized by elemental analysis. For thermogravimetric (TG) analysis, the polymer samples were heated to 700 °C at a heating rate of 10 °C/min under a dry nitrogen atmosphere in a Du Pont Thermal Analyst 2100 system. The pH-sensitive 4VP-*g*-PVDF MF membranes were fabricated by phase inversion¹³ at 25 °C from a NMP solution containing 12 wt % of the respective copolymer, similar to the procedures adopted for the preparation of the AAc-*g*-PVDF MF membranes.¹² The surface composition of copolymer membranes was studied by X-ray photoelectron spectroscopy (XPS). The conditions for the XPS measurements were similar to those reported earlier.¹² Surface elemental stoichiometries were determined from peak area ratios, after correcting with the experimentally determined sensitivity factors, and were reliable to within ±5%. Scanning electron microscopy (SEM) measurements were carried out on a JEOL 6320 scanning electron microscope at an accelerating voltage of 8 kV. Each sample surface was lightly sputtered with gold. The pore sizes and pore size distribution of the pristine PVDF membranes (commercial products of the Millipore Corp., Bedford, MA) and copolymer membranes were measured using a Coulter Porometer (Coulter Electronics Ltd., Luton, U.K.), by the liquid displacement technique.¹² The morphology of the membranes was studied by scanning electron microscopy (SEM). For flux measurements, the membrane was immersed in an aqueous HCl solution of a prescribed pH value and then mounted on the microfiltration cell (Toyo Roshi UHP-25, Tokyo, Japan). An aqueous solution of HCl of the same pH value was added to the cell. NaCl is added to adjust the ionic strength (I) of the acid solutions to 0.1 mol/L.

The chemical structure of the AAc-*g*-PVDF and 4VP-*g*-PVDF copolymer powders was studied by FTIR (FTS135, Bio-Rad Laboratories, Cambridge, MA) in transmission mode. Compared to that of the pristine PVDF, the spectrum of the 4VP-*g*-PVDF copolymers contains a characteristic absorption band for the pyridine groups ($\nu = 1602$ cm⁻¹), associated with the grafted 4VP chains.¹⁴ The ratios of the absorption peak areas at 1602 cm⁻¹ to that at 1120–1280 cm⁻¹ (the absorption band associated with the CF₂ groups of PVDF¹²) are directly related to the bulk graft concentrations of the 4VP side chains in the 4VP-*g*-PVDF copolymers. The FTIR results indicated that the bulk graft concentration increased with the increase in the molar feed ratio of 4VP/PVDF ($[4VP]/[-CH_2CF_2-]$) used for graft copolymerization.

Results and Discussion

The 4VP-*g*-PVDF copolymer exhibits an intermediate thermal stability, when compared to that of the 4-vinylpyridine homopolymer and that of PVDF. A two-step thermal decomposition process was observed for the copolymers. The onset of the first and second major weight loss corresponded, respectively, to that of the 4VP homopolymer (300 °C) and that of PVDF (400 °C). The extent of weight loss for each 4VP-*g*-PVDF copolymer during the first stage of thermal decomposition was

approximately equal to the content of the 4VP segments in the graft copolymers. Similar weight loss behavior was observed for the AAc-*g*-PVDF copolymers.¹²

XPS analyses of the respective copolymer membranes suggest a substantial surface enrichment of the grafted 4VP and AAc polymer side chains. The increase in the graft concentration with the $[4VP]$ or $[AAc]$ to $[-CH_2CF_2-]$ feed ratio is readily indicated by the steady increase in the $-CH-$ peak component intensity and the steady decrease in the CF_2 peak component intensity in the C 1s core-level spectra. The bulk elemental composition (determined by elemental analyses) and the surface elemental composition (determined from the XPS N 1s to C 1s (or C 1s to F 1s) core-level spectral area ratios) for each copolymer membrane were compared. The bulk and surface graft concentration, defined as the number of 4VP or AAc repeat units per repeat unit of PVDF, or the $[-4VP-]/[-CH_2CF_2-]$ and $[-AAc-]/[-CH_2CF_2-]$ ratio, can be readily determined from the $[N]/[C]$ or the $[C]/[F]$ ratio, by taking into account the elemental stoichiometries of the graft and the fluoropolymer chains. The results are summarized in Table 1. For both types of copolymer membranes, the surface graft concentration is always much higher than the bulk graft concentration. Because of the immiscibility of the hydrophilic graft chains and the hydrophobic PVDF chains, as well as the strong interaction of the hydrophilic graft chains with the aqueous medium, surface enrichment of the hydrophilic grafted chains occurs in both types of the copolymer membranes during the phase inversion process in water.

The SEM images, obtained at a magnification of 5000× for the MF membranes cast by the phase inversion technique at 25 °C from the 12 wt % NMP solutions of the pristine PVDF powders and three 4VP-*g*-PVDF copolymers ($([-4VP-]/[-CH_2CF_2-])_{bulk} = 0.04, 0.07, \text{ and } 0.08$, respectively), are shown in Figure 2. The membranes cast from the NMP solutions of the 4VP-*g*-PVDF copolymer samples have a higher porosity than that cast from the NMP solution of the pristine PVDF.

The pore sizes of the commercial PVDF MF membranes and the various AAc-*g*-PVDF and 4VP-*g*-PVDF membranes were measured on the Coulter Porometer II apparatus. The results are given in Table 1. The pore size distribution of the present AAc-*g*-PVDF and 4VP-*g*-PVDF membranes are similar to those of the commercial PVDF membranes with standard pore diameters (d) between 0.45 and 0.65 μm (see Table 1). Thus, the commercial PVDF membranes with $d = 0.45$ and $d = 0.65$ μm were selected as the pristine PVDF MF membranes for the comparative flux study in the

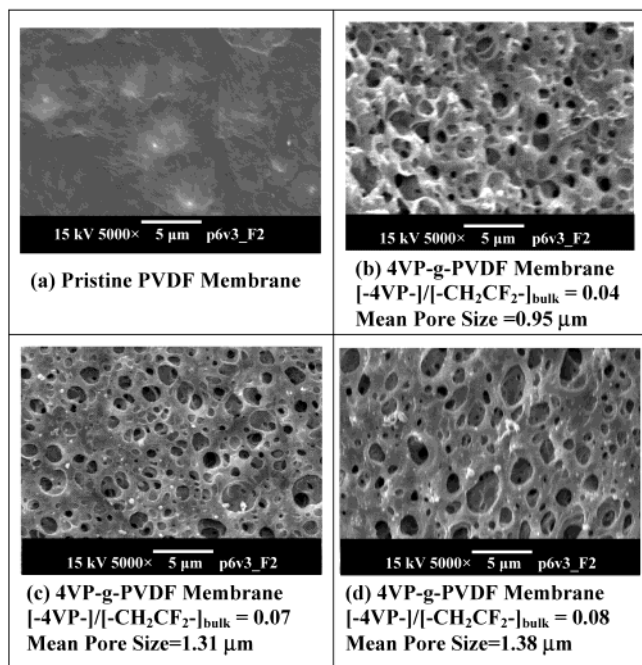


Figure 2. SEM micrographs of the MF membranes cast by phase inversion from 12 wt % NMP solution of (a) the pristine PVDF and the 4VP-*g*-PVDF copolymers of graft concentrations ($[-4VP-]/[-CH_2CF_2-]_{bulk}$ ratios) of (b) 0.04, (c) 0.07, and (d) 0.08.

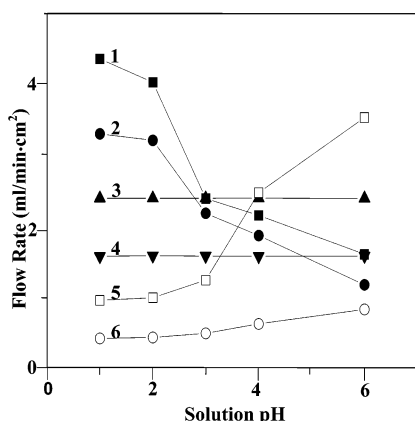


Figure 3. pH-dependent water permeability through the pristine PVDF, AAc-*g*-PVDF and 4VP-*g*-PVDF MF membranes. Curves 1 and 2 are obtained from two AAc-*g*-PVDF MF membranes with graft concentrations ($[-AAc-]/[-CH_2CF_2-]_{surface}$ ratios) of 0.97 and 0.13, respectively; Curves 3 and 4 are from fluxes through the commercial PVDF membranes (standard pore diameters: $d = 0.65$ and $0.45 \mu m$, respectively); Curves 5 and 6 are obtained from two 4VP-*g*-PVDF MF membranes with graft concentrations ($[-4VP-]/[-CH_2CF_2-]_{surface}$ ratios) of 0.55 and 0.13, respectively. (The mean pore sizes for all the membranes are given in Table 1).

present work. The flux of aqueous solutions of different pH values through the AAc-*g*-PVDF, the 4VP-*g*-PVDF, and the pristine PVDF MF membranes were investigated. The results are shown in Figure 3. The AAc-*g*-PVDF and the 4VP-*g*-PVDF MF membranes were cast from the 12 wt % NMP solution of the respective copolymer. Differing from the flux through the pristine PVDF MF membrane, the flux of the aqueous solution through the AAc-*g*-PVDF and 4VP-*g*-PVDF MF membranes exhibits a pH-dependent behavior. Because of the nonionizability of the polymer chains in the pristine PVDF MF membranes, the polymer chain conformation

and the membrane pore dimension will remain constant at all pH values. On the other hand, however, the permeability through the AAc-*g*-PVDF MF membranes decreases with the increase in the solution pH value from 1 to 6, with the most drastic decrease being observed at solution pH values between 2 and 4. The changes in permeability in response to changes in solution pH may be attributed to the changes in the conformation of the AAc side chains on the surfaces (especially those on the pore surfaces). As a weak acid ($pK_a = 4.3$), the carboxylic groups of the AAc-*g*-PVDF copolymer can be ionized readily, or deprotonated, to become negatively charged. With increasing pH values ($pH > 3$), most of the carboxylic groups are transformed into carboxylic ions. Strong electrostatic repulsion among the carboxylic ions, together with their strong interaction with aqueous solution, force AAc polymer side chains to adopt a highly extended conformation. The extension of the AAc side chains into the pores reduces the effective pore dimensions and results in a reduced permeability of the aqueous solution through the MF membranes.¹⁵

In contrast to the pH-independent nature of the flux through the pristine PVDF MF membrane and differing from the pH-sensitive flux behavior through the AAc-*g*-PVDF MF membrane, the flux of the aqueous solution through the 4VP-*g*-PVDF MF membranes exhibits a reversed pH-dependent behavior. The flow rate of the aqueous solution through the 4VP-*g*-PVDF MF membranes increases with the increase in solution pH from 1 to 6. As a weak base, the pendent pyridine groups of the grafted 4VP side chains are protonated and become complexed in an acid solution. The resulting ionic character and the electrostatic repulsion among the positively charged pyridinium nitrogen atoms overcome the hydrophobic interactions among the alkyl segments of the chains. The uncoiling of the polymer side chains and their interactions with the aqueous solution lead to an extended conformation in the pores. As a result, the effective pore dimensions and thus the permeability of the aqueous solution through MF membrane are reduced. For both types of the MF membranes, the magnitude of the pH-dependent change in flux is enhanced by the increase in graft concentration.

The pyridine groups on the 4VP side chains can become involved in two types of interactions, viz., hydrogen bonding and protonation (proton-transfer interaction), that lead to the observed pH sensitivity of the flux through the 4VP-*g*-PVDF MF membrane. XPS was employed to study the variation in the chemical state of the nitrogen after the 4VP-*g*-PVDF MF membrane has been exposed to acidic solutions of different pH values for 5 min. The resulting N 1s core-level spectra are shown in Figure 4. For the nitrogen-containing species, such as pyridine and imidazole, hydrogen bonding with the proton-donating species, such as phenols, carboxylic acids, inorganic acids, and water, occurs readily.^{16–20} All XPS spectra can be curve-fitted with three components using the following approaches. The peak component at the binding energy (BE) of about 398.5 eV is assigned to the imine ($-N=$) moiety of the pyridine rings, the peak component at about 399.5 eV is assigned to the hydrogen-bonded imine, and the peak component at about 400.8 eV is assigned to the protonated pyridinium ions. The latter species has been reported to undergo a positive BE shift of 2.1–2.5 eV from the neutral pyridine nitrogen.^{21,22}

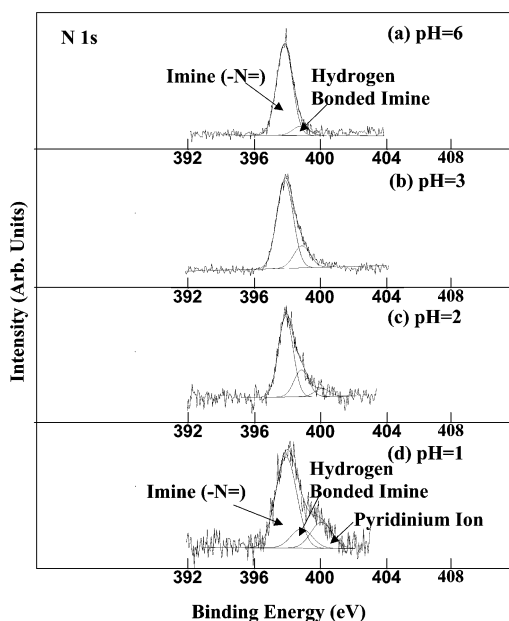


Figure 4. XPS N 1s core-level spectra of four MF membranes cast by phase inversion from a 12 wt % NMP solution of the 4VP-*g*-PVDF copolymer ($[-4VP-]/[-CH_2CF_2-]_{\text{surface}} = 0.55$) and after being immersed for 5 min in aqueous solutions of different pH value: (a) pH = 6, (b) pH = 3, (c) pH = 2, and (d) pH = 1.

Figure 4 clearly indicates that, when the proton concentration is low or when the pH value is higher than 2, the main form of interaction is hydrogen bonding. The percentage of N atoms involved in the hydrogen bonding increases from 9% to 21% when the pH value of the solution decreases from 6 to 3. When the pH value of the solution is decreased to 2, protonation of pyridine becomes significant. The percentages of imine groups involved in hydrogen bonding and protonation are 21% and 7%, respectively. When the solution pH is further decreased to 1, the main form of interaction switches from hydrogen bonding to protonation or formation of the pyridinium ions. The amount of protonated imine groups increases to 19%, while that of imine groups involved in hydrogen bonding is reduced to 14%.

Conclusions

Acrylic acid and 4-vinylpyridine had been graft-copolymerized onto the ozone-preactivated PVDF main chains in solution. XPS analyses of the resulting AAc-*g*-PVDF and 4VP-*g*-PVDF MF membranes cast by phase

inversion in water revealed a significant surface enrichment of the hydrophilic components. The fluxes of the aqueous solutions through both the AAc-*g*-PVDF and 4VP-*g*-PVDF MF membranes were pH-dependent, but in an opposite manner. The phenomena arose from the weak acid and base nature of the respective AAc and 4VP graft chains. The interactions between the pyridine groups and the aqueous acid solutions included hydrogen bonding and pyridine protonation. When the proton concentration was low, hydrogen bonding predominated. Pyridine protonation became significant only when the proton concentration was higher than 0.01 M.

References and Notes

- (1) Khayet, M.; Matsuura, T. *Ind. Eng. Chem. Res.* **2001**, *3*, 379.
- (2) Hietala, S.; Maunu, S. L.; Sundholm, F. *Macromolecules* **1999**, *32*, 788.
- (3) Fan, L.; Harris, J. L.; Roddick, F. A.; Booker, N. A. *Water Res.* **2001**, *35*, 4455.
- (4) Brophy, P. D.; Mottes, T. A.; Kudelka, T. L.; McBryde, K. D.; Gradner, J. J.; Maxwold, N. J.; Bunchman, T. E. *J. Kidney Dis.* **2001**, *38*, 173.
- (5) Osanai, S.; Nakamura, K. *Biomaterials* **2000**, *21*, 867.
- (6) Ito, Y.; Ochiai, Y.; Park, Y. S.; Imanishi, Y. *J. Am. Chem. Soc.* **1997**, *119*, 1619.
- (7) Iwata, H.; Hirata, I.; Ikada, Y. *Macromolecules* **1998**, *31*, 3671.
- (8) Hester, J. F.; Banerjee, P.; Mayes, A. M. *Macromolecules* **1999**, *32*, 1643.
- (9) Nunes, S. P.; Sforca, M. L.; Peinemann, K. V. *J. Membr. Sci.* **1995**, *106*, 49.
- (10) Boutevin, B.; Robin, J.; Serdani, A. *Eur. Polym. J.* **1992**, *28*, 1507.
- (11) Niemoeller, H.; Scholz, H.; Goetz, B.; Ellinghorst, J. *J. Membr. Sci.* **1988**, *36*, 385.
- (12) Ying, L.; Wang, P.; Kang, E. T.; Neoh, K. G. *Macromolecules* **2002**, *35*, 673.
- (13) Fried, J. R. *Polymer Science and Technology*; Prentice Hall: Upper Saddle River, NJ, 1995; p 450.
- (14) Halil, I. U.; Oya, S. *J. Appl. Polym. Sci.* **1996**, *62*, 1165.
- (15) Tonge, S. R.; Tighe, B. J. *Adv. Drug Delivery Rev.* **2001**, *53*, 109.
- (16) Urzua, M.; Gargallo, L.; Radic, D. *J. Appl. Polym. Sci.* **2002**, *84*, 1245.
- (17) Goh, S. H.; Lee, S. Y.; Dai, J.; Tan, K. L. *Polymer* **1996**, *37*, 5305.
- (18) Zhou, X.; Goh, S. H.; Lee, S. Y.; Tan, K. L. *Appl. Surf. Sci.* **1997**, *119*, 60.
- (19) Schlucker, S.; Heid, M.; Singh, R. K.; Asthana, B. P.; Popp, J.; Kiefer, W. Z. *Phys. Chem.* **2002** (Part 3), *216*, 267.
- (20) Houben, L.; Schoone, K.; Maes, G. *Vibr. Spectrosc.* **1996**, *10*, 147.
- (21) Tan, K. L.; Tan, B. T. G.; Kang, E. T.; Neoh, K. G. *J. Mol. Electron.* **1990**, *6*, 5.
- (22) Li, L.; Chan, C. M.; Weng, L. T.; Xiang, M. L.; Jiang, M. *Macromolecules* **1998**, *31*, 7248.

MA025566H